Neurobiology of Disease

Effects of Peritoneal Sepsis on Rat Central Osmoregulatory Neurons Mediating Thirst and Vasopressin Release

Jerneja Stare,[1,2]* Shidasp Siami,[3]* Eric Trudel,[1] Masha Prager-Khoutorsky,[1] Tarek Sharshar,[4,5] and Charles W. Bourque[1,2]

[1]Centre for Research in Neuroscience, Research Institute of the McGill University Health Centre, Montreal, Quebec, Canada H3G 1A4, [2]Department of Physiology, McGill University, Montreal, Quebec, Canada H3G 1Y6, [3]Department of Intensive Care Medicine, Sud Essonne Hospital, F-91152 Étampes, France, [4]General Intensive Care Medicine, Raymond Poincaré Hospital, Garches, 92380 Paris, France, and [5]Department of Histopathology and Animal Models, Pasteur Institute, F-75015 Paris, France

Sepsis is a life-threatening condition caused by the systemic inflammatory response to a bacterial infection. Although much is known about the cellular and molecular changes that characterize the peripheral inflammatory response to sepsis, almost nothing is known of the neuronal changes that cause associated perturbations in the central control of homeostasis. Osmoregulation is one of the key homeostatic systems perturbed during sepsis. In healthy subjects, systemic hypertonicity normally excites osmoreceptor neurons in the organum vasculosum laminae terminalis (OVLT), which then activates downstream neurons that induce a parallel increase in water intake and arginine vasopressin (AVP) secretion to promote fluid expansion and maintain blood pressure. However, recent studies have shown that the early phase of sepsis is associated with increased AVP levels and suppressed thirst. Here we examined the electrophysiological properties of OVLT neurons and magnocellular neurosecretory cells (MNCs) in acute *in vitro* preparations obtained from rats subjected to sham surgery or cecal ligation and puncture (CLP). We found that the intrinsic excitability of OVLT neurons was not affected significantly 18–24 h after CLP. However, OVLT neurons in CLP rats were hyperpolarized significantly compared with shams. Moreover, a reduced proportion of these cells displayed spontaneous electrical activity and osmoresponsiveness in septic animals. In contrast, the osmoresponsiveness of MNCs was only attenuated by CLP, and a larger proportion of these neurons displayed spontaneous electrical activity in septic animals. These results suggest that acute sepsis disrupts centrally mediated osmoregulatory reflexes through differential effects on the properties of neurons in the OVLT and supraoptic nucleus.

Key words: **osmoreceptor; sepsis; thirst; vasopressin**

Significance Statement

Sepsis is a life-threatening condition caused by the systemic inflammatory response to bacterial infection. Although the early phase of sepsis features impaired thirst and enhanced vasopressin release, the basis for these defects is unknown. Here, we show that cecal ligation and puncture (CLP) in rats impairs the osmoresponsiveness of neurons in the organum vasculosum lamina terminalis (OVLT; which drives thirst) and attenuates that of neurosecretory neurons in the supraoptic nucleus (SON; which secrete oxytocin and vasopressin). Notably, we found that OVLT neurons are hyperpolarized and electrically silenced. In contrast, CLP increased the proportion of SON neurons displaying spontaneous electrical activity. Therefore, CLP affects the properties of osmoregulatory neurons in a manner that can affect systemic osmoregulation.

Introduction

Sepsis is a life-threatening condition resulting from an excessive systemic inflammatory response to bacterial infection (Cinel and Opal, 2009; Angus and van der Poll, 2013). It is commonly complicated by multiple organ failure and circulatory shock (hypotension and tissue hypoperfusion), which is associated with a high mortality rate (~50%). Survivors of the condition com-

Received Dec. 28, 2013; revised July 27, 2015; accepted July 28, 2015.

Author contributions: T.S. and C.W.B. designed research; J.S., S.S., E.T., and M.P.-K. performed research; J.S., S.S., and C.W.B. analyzed data; J.S. and C.W.B. wrote the paper.

This work was supported by Canadian Institutes of Health Research (CIHR) Operating Grant MOP-9939 to C.W.B., who was also recipient of a James McGill Research Chair. J.S. was a recipient of the CIHR Frederick Banting and Charles Best Canada Graduate Scholarship–Doctoral Award. The Research Institute of the McGill University Health Center is supported by the Fonds de Recherche du Québec–Santé.

The authors declare no competing financial interests.

*J.S. and S.S. contributed equally to this work.

Correspondence should be addressed to Charles Bourque, Division of Neurology L7–216, Montreal General Hospital, 1650 Cedar Avenue, Montreal, QC, Canada H3G 1A4. E-mail: charles.bourque@mcgill.ca.

DOI:10.1523/JNEUROSCI.5420-13.2015

 0270-6474/15/3512188-10$15.00/0

monly suffer from life-long ailments related to organ damage, including brain dysfunction (Lazosky et al., 2010; Sonneville et al., 2013; Ziaja, 2013). Sepsis is a complex syndrome (Angus and van der Poll, 2013) that features many centrally mediated symptoms, including the establishment of sickness behavior (Bauhofer et al., 2004), the generation of appropriate and inappropriate neuroendocrine responses (Giusti-Paiva and Santiago, 2010; Kanczkowski et al., 2013), and alterations in autonomic output that contribute to hypotension and hypovolemia (Pancoto et al., 2008). Although much information is available concerning the peripheral immune responses associated with sepsis (Cinel and Opal, 2009), little is known of the changes in neuronal excitability that mediate the central manifestations of the disorder.

As noted above, sepsis is associated with sickness behavior, a syndrome that features an inhibition of thirst (Hart, 1988). Notably, systemic infusion of bacterial endotoxin has been shown to inhibit water intake provoked by dehydration (Calapai et al., 1990; Wang and Evered, 1993; Nava and Carta, 2000), a stimulus that promotes both hypovolemia and hyperosmolality and therefore potently stimulates thirst (Johnson, 2007). Although hypovolemia and hyperosmolality stimulate thirst via distinct visceral sensory systems (Antunes-Rodrigues et al., 2004), the inhibitory effect of endotoxin on dehydration-induced thirst has been shown to involve the preoptic nucleus (Calapai et al., 1994), an area encompassing the primary osmoreceptor of the brain: the organum vasculosum laminae terminalis (OVLT; Johnson and Buggy, 1978). Therefore, reduced water intake during sepsis may specifically involve osmotic thirst and be attributable to an inhibition of OVLT neurons.

Under normal conditions, excitation of OVLT neurons during systemic hypertonicity causes an increase in thirst via projections to the prefrontal cortex (McKinley et al., 2006; Hollis et al., 2008) and a parallel increase in arginine vasopressin (AVP; antidiuretic hormone) release via excitatory projections to hypothalamic magnocellular neurosecretory cells (MNCs; Richard and Bourque, 1995; Bourque, 2008; Trudel and Bourque, 2010). Therefore, a defect in the osmotic activation of OVLT neurons would be expected to impair AVP release as well. However, previous work has shown that circulating levels of AVP are elevated during the early stages of sepsis in both humans (Sharshar et al., 2003) and rats (Pancoto et al., 2008; Athayde et al., 2009; Oliveira-Pelegrin et al., 2009). The mechanism by which water intake and AVP responses become dissociated during sepsis remain unknown. In this study, we examined whether sepsis induced by cecal ligation and puncture (CLP) inhibits fluid intake stimulated by systemic hyperosmolality in rats, and we compared the effect of this condition on the electrophysiological properties of OVLT neurons and MNCs of the supraoptic nucleus (SON).

Materials and Methods

Animals. All experiments were performed on male Long–Evans rats (80–120 g) obtained from Charles River Laboratories according to protocols approved by the Facility Animal Care Committee of McGill University. Animals were housed under 12 h light/dark conditions, and food and water were provided *ad libitum*, except in experiments in which the drinking solution was replaced by 2% NaCl.

CLP. Sepsis was induced in rats using the CLP method as described by Rittirsch et al. (2009). Surgeries were performed on animals anesthetized with vaporized isoflurane (Pharmaceutical Partners of Canada) at 2–5% in a stream of O_2 (0.4–1.5 L/min). After a 3–4 cm midline laparotomy, the cecum was exposed and ligated below the ileocecal junction with a 3.0 silk suture (Ethicon), isolating ~65% of the cecum. It was then punctured twice with an 18 gauge needle—once at the proximal end and once at the distal end—and a small amount of fecal matter was extruded

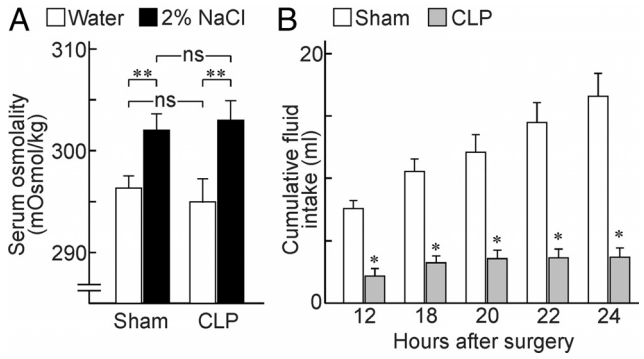

Figure 1. CLP-induced sepsis inhibits osmotic thirst. ***A***, Bar graphs show mean ± SEM values of serum osmolality 18–24 h after sham or CLP surgery in rats provided with water (sham, $n = 7$ rats; CLP, $n = 4$ rats) or 2% NaCl as drinking fluid (sham, $n = 7$ rats; CLP, $n = 5$ rats). ***B***, Bar graphs show mean ± SEM cumulative fluid intake in sham ($n = 6$ rats) and CLP ($n = 4$ rats) rats given access to 2% NaCl. *$p < 0.05$; **$p < 0.01$; ns, not significant.

inside the peritoneal cavity. After these punctures, the cecum was repositioned into the abdominal cavity, and the overlaying muscles and skin were treated with a topical analgesia mixture (0.4% lidocaine from AlvedaPharma; 0.2% bupivacaine from Hospira) and sutured closed (with 3.0 monofilament nylon suture and 3.0 silk suture, respectively; Ethicon). The animals were then injected subcutaneously with sterile saline (0.5 ml/10 g body weight), placed in fresh cages individually, and monitored for recovery before being returned to the housing room. Sham control rats underwent the same procedure, without ligation or puncture of the cecum. All rats were killed 18–24 h after the operation and necropsied to ensure the quality of the CLP or sham surgery. CLP rats that did not develop stereotypical septic symptoms according to an in-house monitoring scale based on the study by Rittirsch et al. (2009), or developed secondary infections or an obstructed bowel, were not used for experiments.

Fluid intake measurements. Drinking behavior was quantified by using drip-proof sipper sacs (Edstrom Industries). Sacs were filled with either water or 2% NaCl solution, weighed in grams, and placed into the rats' cages at the time of surgery (time point 0). After surgery, the animals were returned to the housing room, and the sipper sacs were weighed 12, 18, 20, 22, and 24 h after surgery. Data from septic animals that died before 24 h after surgery were included, but values at time points after death were capped at the last recorded measurement, whereas data were excluded in cases of sipper sac leakage. Fluid intake was reported in milliliters at the conversion rate of 1.0151 g/ml for water and 1.0258 g/ml for 2% NaCl.

Serum osmolality. Blood samples were collected by cardiac puncture from rats under 2–5% isoflurane anesthesia. Approximately 1–2 ml of blood was collected per animal and placed on ice (30–90 min). Blood samples were then spun at 8000 rpm for 5 min in a Spectrafuge 24D centrifuge (Labnet International). The serum samples were collected into fresh microcentrifuge tubes and stored at 4°C before processing. Serum osmolality values were averaged over three to five measurements using a freezing point osmometer (model 3320; Advanced Instruments).

Histological analysis and image processing. For localization of the OVLT region, which lacks a blood–brain barrier, animals were anesthetized with isoflurane and injected intravenously with 0.5 ml of a 1% solution of Evans Blue (Sigma) dissolved in PBS. After 30 min, the animals were killed by decapitation, and the brain was removed and fixed by immersion for 48 h in 4% paraformaldehyde dissolved in PBS. Explants were then prepared as described below and photographed in whole mount to identify the OVLT region.

For cell counts, animals were anesthetized with isoflurane and perfused (transcardiac route) with 10 ml of PBS, followed by 300 ml of 4% paraformaldehyde in PBS. Coronal sections were cut on a vibratome (50 μm thickness), and the eight consecutive sections lying rostral to (and one including) the preoptic recess of the third ventricle were retained for staining and analysis. The sections were blocked with 10% normal goat serum (in PBS containing 0.3% Triton X-100) and incubated overnight

with a chicken polyclonal anti-NeuN antibody (1:500 in PBS; EMD Millipore). Sections were then washed and incubated in goat anti-chicken secondary antibody (Alexa Fluor 568 conjugated; 1:200 in PBS; Life Technologies) and phalloidin (Alexa Fluor 647 conjugated; 1:300; Life Technologies) and mounted on coverslips using SlowFade Gold Antifade reagent (Life Technologies). z-Stack images were collected at 11 × 5 μm steps using an Olympus FV1000 confocal microscope equipped with a 20×, 0.85 numerical aperture oil-immersion lens.

Acquired z-stack images were thresholded for background and counted blind using Imaris 6.4 (Bitplane). Overlapping image stacks were stitched using XuvTools v2 (Free Software Foundation) in cases in which multiple frames were required to cover the entirety of the OVLT area. Briefly, two rectangular boxes covering a total area of 400 μm × 300 μm × 9 voxels were drawn over the OVLT region using actin-stained blood vessels and cells as location references. Spheres representing the NeuN-stained nuclei were rendered and automatically quantified by the program within each cube after thresholding for diameter (7.030 μm) and spot "quality" feature (above 220 or 230 units). Individual 3D-rendered samples were then adjusted manually and verified for adherence to the unbiased brick-counting rules. Maximum projection images for presentation were produced using NIH ImageJ software (version 1.46r).

Extracellular recording in hypothalamic explants. Animals were decapitated, and the brain was removed from the cranial vault. Hypothalamic explants were prepared as described previously using a razor blade and pinned ventral side up to the Sylgard base of a perfusion chamber in which carbogenated (95% O_2, 5% CO_2) artificial CSF (ACSF; 32°C) was delivered over the region of interest at a rate of ~1–1.5 ml/min (Stachniak et al., 2012). The ACSF comprised the following (in mM): 120 NaCl, 4 KCl, 1.46 $MgCl_2$, 29.95 $NaHCO_3$, 1 $CaCl_2$, 1.23 NaH_2PO_4, and 10 D-glucose, pH 7.35. A slightly higher concentration of external K^+ was used (4 mM) for extracellular recordings than for whole-cell recordings in slices (3 mM, see below) to facilitate spontaneous firing. Osmolality was adjusted as required by the addition of mannitol. Extracellular recording microelectrodes pulled on a pipette puller (P-87; Sutter Instruments) and filled with 1 M NaCl (10–20 MΩ) were advanced using an IVM micromanipulator (Scientifica) at an advance rate of 0.4 μm/s. Voltage signals recorded via an Axoclamp-2A (Molecular Devices) were filtered at 0.5–1.2 kHz and amplified (500×) before capture using Clampex 10 software (Molecular Devices). When single-unit action potential (AP) firing (signal-to-noise ratio >3) was detected, electrode advance was paused, and the average rate of basal AP firing was determined over a period of 1 min. Cells that completely stopped firing soon after being encountered were counted but were assigned a value of 0 Hz for basal firing. Cells that continued to fire for >1 min were selected for additional testing to a hyperosmotic stimulus. The effects of a 5 min hyperosmotic stimulation (+15 mOsm/kg) on OVLT neurons were assessed by subtracting the rate of basal firing from the average rate of AP firing recorded during the last 60 s of the stimulus. Neurons in the SON were tested for their osmoresponsiveness using a +20 mOsm/kg stimulus. Basal firing rate was measured 30 s before the stimulus, and osmotically induced firing was quantified as the maximum average rate observed during the 30 s interval that displayed the greatest increase in firing during the stimulus.

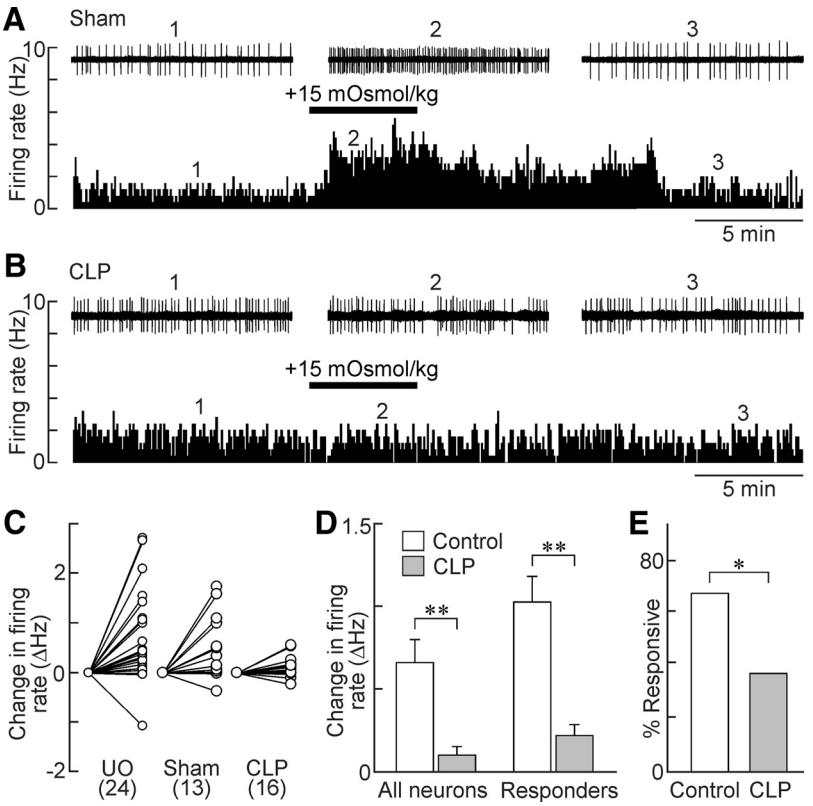

Figure 2. Osmosensitivity of OVLT neurons is lost in CLP rats. ***A***, Ratemeter records (5 s bin width) showing the firing rate of a single OVLT neuron in an explant prepared from a sham rat. Note the reversible excitatory effect of the hyperosmotic stimulus (bar). Traces above the ratemeter plot show excerpts of the raw single-unit activity recorded at the time points indicated by the numbers. ***B***, Response of an OVLT neuron recorded from a CLP rat (layout as in ***A***). ***C***, Two-point plots show the changes in firing rate induced by hyperosmotic stimulation in all of the OVLT neurons tested in unoperated (UO), sham and CLP rats (UO 24 neurons/9 rats; sham, 13 neurons/7 rats; CLP, 16 neurons/5 rats). ***D***, Bar graphs show mean ± SEM changes in firing rate induced by hypertonicity in all of the OVLT neurons tested in control rats (UO + sham; 37 neurons/16 rats) and CLP (16 neurons/5 rats) or in the specific subset of OVLT neurons that showed at least a 15% increase in firing rate (responders: control, 25 neurons/16 rats; CLP, 6 neurons/5 rats). ***E***, Bar graphs show proportions of responders in controls (25 neurons/16 rats) and CLP animals (6 neurons/5 rats). $*p < 0.05$; $**p < 0.01$.

Extracellular recordings from the SON in explants were not obtained from MNCs identified specifically as AVP containing. However, the recordings were made in the ventral, AVP-rich zone of the nucleus (Stachniak et al., 2012), and many of the cells displayed phasic firing, a specific characteristic of AVP neurons (Brimble and Dyball, 1977).

Whole-cell recordings in hypothalamic slices. Angled hypothalamic slices were obtained as described previously (Trudel and Bourque, 2010; Stachniak et al., 2012). Briefly, brains were placed in ice-cold (0–4°C) carbogenated ACSF containing the following (in mM): 120 NaCl, 3 KCl, 1.23 NaH_2PO_4, 1.48 $MgCl_2$, 2 $CaCl_2$, 26 $NaHCO_3$, and 10 D-glucose. The dorsal surface of the brain was glued to an angled (35°) mounting block, and a single 400 μm slice just caudal to the optic chiasma was cut on a vibratome (VT1200; Leica), transferred to a recording chamber, and perfused at ~2 ml/min with carbogenated ACSF at 30–32°C.

Patch pipettes (3–5 MΩ) made using a P-87 puller (Sutter Instruments) were filled with an internal solution containing the following (in mM): 110 K-gluconate, 1 $MgCl_2$, 10 KCl, and 10 HEPES, pH 7.4 with KOH (282 mOsm/kg). Series resistance was 5–15 MΩ. Whole-cell current and voltage recorded using an Axopatch-1D amplifier (Molecular Devices) were digitized using Clampex and analyzed using Clampfit 10 software (Molecular Devices). Resting membrane potential (RMP) was defined as the membrane voltage observed when zero current was being injected. AP threshold was defined arbitrarily as the voltage from which the rate of rise exceeded 50 V/s during the upstroke of the AP. Rheobase was defined as the steady-state voltage from which APs were observed to occur in response to slow current injection. Conductance was deter-

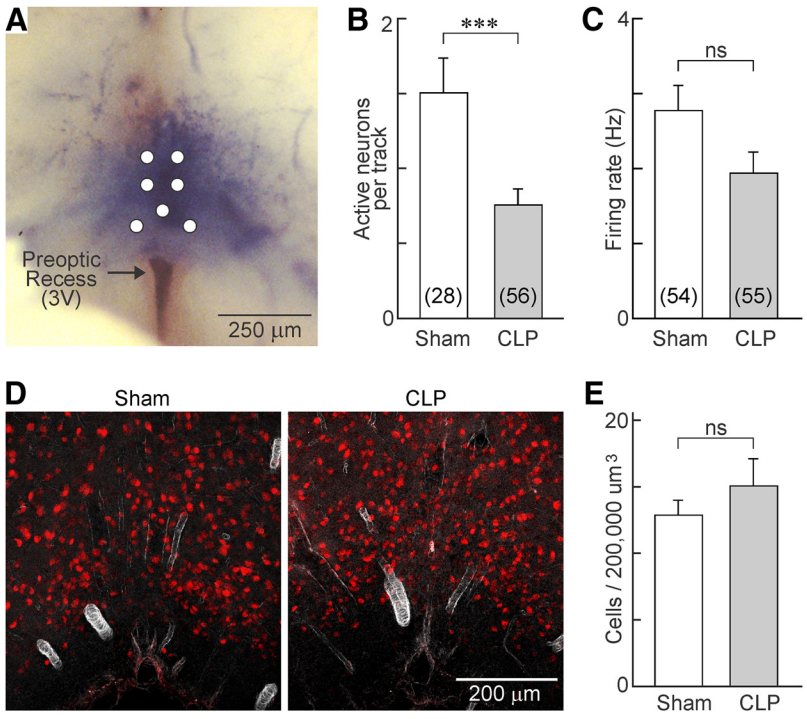

Figure 3. CLP reduces the density of cells showing spontaneous electrical activity but not neuron density in OVLT. ***A***, Whole-mount photograph showing the ventral surface of the brain in a hypothalamic explant prepared from a rat injected intravenously with 1% Evans Blue. Top is rostral, and bottom is caudal. Note that the dye is localized to the parenchyma of the tissue that lies immediately rostral to the anterior edge of the preoptic recess of the third ventricle (3V). The white circles show the positions at which microelectrodes were inserted. ***B***, Bar graphs show the mean ± SEM density of spontaneously active neurons observed in the OVLT of sham and CLP animals ($n = 28$ tracks/4 rats and $n = 56$ tracks/8 rats, respectively). ***C***, Bar graphs show the mean ± SEM steady-state firing rate of spontaneously active OVLT neurons in sham ($n = 54$ neurons/10 rats) and CLP ($n = 55$ neurons/8 rats) animals. ***D***, Immunofluorescence micrograph showing staining for the neuronal marker NeuN (red) in representative coronal sections through the OVLT of sham ($n = 26$ sections/3 rats) and CLP ($n = 23$ sections/3 rats) animals. ***E***, Bar graphs show the mean ± SEM density of NeuN-positive cells counted per unit volume in the OVLT of sham and CLP rats. ***$p < 0.005$; ns, not significant.

mined as the slope of a line fitted by linear regression to the current–voltage (I–V) relation in the voltage range below AP threshold (i.e., −70 to −50 mV for OVLT neurons and −60 to −40 mV for SON neurons). For SON neurons, a subset of the data was obtained from current-clamp recordings in which conductance was determined to be the inverse of input resistance ($\Delta I/\Delta V$) between −60 and −40 mV. Although whole-cell recordings in the SON were not obtained from MNCs specifically identified as AVP containing, these were made from cells along the ventral, AVP-rich zone of the nucleus (Stachniak et al., 2012).

Statistics. All values are reported as mean ± SEM. Means of groups were compared for differences using SigmaPlot 12 (Systat Software) by applying, as appropriate, Student's t test, paired t test, one-way ANOVA, or two-way ANOVA. When significant differences were reported by ANOVA ($p < 0.05$), *post hoc* Tukey's or Holm–Sidak tests were applied to identify the groups that differed and to compute F and p values. Proportions of responsive cells in sham and CLP animals were compared using the χ^2 test performed with SigmaPlot 12. Slopes of I–V relations used to measure membrane conductance were obtained by linear regression, and slopes were compared using Prism 5 (GraphPad Software). Differences between mean values were considered significant at $p < 0.05$.

Results

Acute sepsis inhibits osmotic thirst

To examine the effects of peritoneal sepsis on thirst behavior, rats were subjected to CLP or sham surgery, returned to their cages, and provided *ad libitum* access to drinking fluid consisting of either water or 2% NaCl. Ingestion of 2% NaCl for a period of 24 h causes a rise in serum osmolality without affecting hematocrit (i.e., blood volume; Jones and Pickering, 1969), thus providing an effective procedure to stimulate central osmoreceptors (OVLT neurons). Basal serum osmolality measured 18–24 h after surgery was not significantly different when rats were given *ad libitum* access to water (sham, 295.9 ± 1.6 mOsm/kg, $n = 7$; CLP, 295.0 ± 2.2 mOsm/kg, $n = 4$; two-way ANOVA, Holm–Sidak test, $p = 0.756$; Fig. 1*A*). However, serum osmolality increased significantly in rats given access to 2% NaCl drinking solution ($F_{(1,19)} = 14.475$, $p = 0.001$), and there was no statistical difference between the mean serum osmolality reached at end point for both types of surgery (sham, 302.0 ± 1.6 mOsm/kg, $n = 7$; CLP, 303.0 ± 1.9 mOsm/kg, $n = 5$; $p = 0.698$; Fig. 1*A*). Despite the increase in serum osmolality experienced by the CLP rats receiving 2% NaCl, cumulative fluid intake in this group was significantly lower than in shams (end values: sham, 16.4 ± 1.8 ml, $n = 6$; CLP, 4.2 ± 0.58 ml, $n = 4$; $p = 0.00082$; Fig. 1*B*).

Acute sepsis impairs osmotic detection in OVLT neurons

The results presented above indicate that osmotically induced thirst is impaired during sepsis. Therefore, we examined the effects of CLP on the responsiveness of OVLT neurons to hyperosmotic stimulation in superfused hypothalamic explants. Increasing the osmolality of the ACSF by addition of 15 mM mannitol caused a reversible excitation of OVLT neurons in explants prepared from either unoperated (0.74 ± 0.19 Hz, $n = 24$ cells; $p = 0.000809$, paired t test) or sham (0.51 ± 0.18 Hz, $n = 13$ cells; $p = 0.0154$, paired t test) animals but not those from rats having undergone the CLP procedure (0.10 ± 0.05 Hz, $n = 16$ cells; $p = 0.0719$, paired t test; Fig. 2*A–D*). Because no significant difference was observed in the responsiveness of unoperated and sham animals ($p = 0.611$, t test), the datasets were pooled into a single "control" group. As shown in Figure 2*D*, the reduced osmoresponsiveness of OVLT neurons observed in CLP rats compared with controls was statistically significant both when all of the neurons tested were considered together (control, 0.66 ± 0.12 Hz vs CLP, 0.10 ± 0.18 Hz; $p = 0.01$) and when only OVLT neurons deemed osmoresponsive (i.e., those showing increases in firing >15%) were compared (control, 1.03 ± 0.14 Hz vs CLP, 0.22 ± 0.24 Hz; $p = 0.004$; $F_{(1,83)} = 15.598$, two-way ANOVA and Holm–Sidak *post hoc* test). Moreover, there was a statistically significant reduction in the proportion of osmotically responsive neurons in the CLP group when compared with controls (controls, 67.6%; CLP, 37.5%; $p = 0.04$, χ^2 test; Fig. 2*E*).

Acute sepsis silences a subset of OVLT neurons

We next examined whether sepsis affected the overall density of spontaneously active neurons that could be detected in the OVLT of sham and CLP animals under isotonic conditions. To this end, a microelectrode was placed on the ventral surface of hypotha-

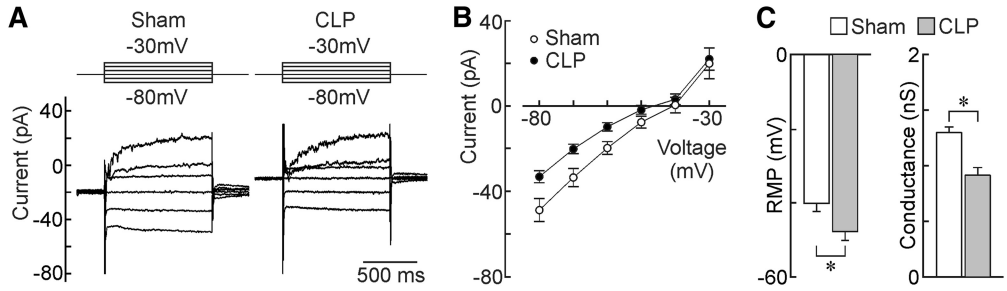

Figure 4. Effects of sepsis on the membrane properties of OVLT neurons. ***A***, Whole-cell membrane current responses (bottom) to voltage commands (top) recorded from OVLT neurons in hypothalamic slices. Each set of traces shows the average responses generated by the entire set of sham ($n = 23$ neurons/3 rats) and CLP ($n = 22$ neurons/3 rats) neurons studied. ***B***, Average *I–V* plots obtained from the corresponding cells. ***C***, Bar graphs show mean ± SEM values of RMP (i.e., voltage at $I = 0$) and conductance measured from the same cells. *$p < 0.05$.

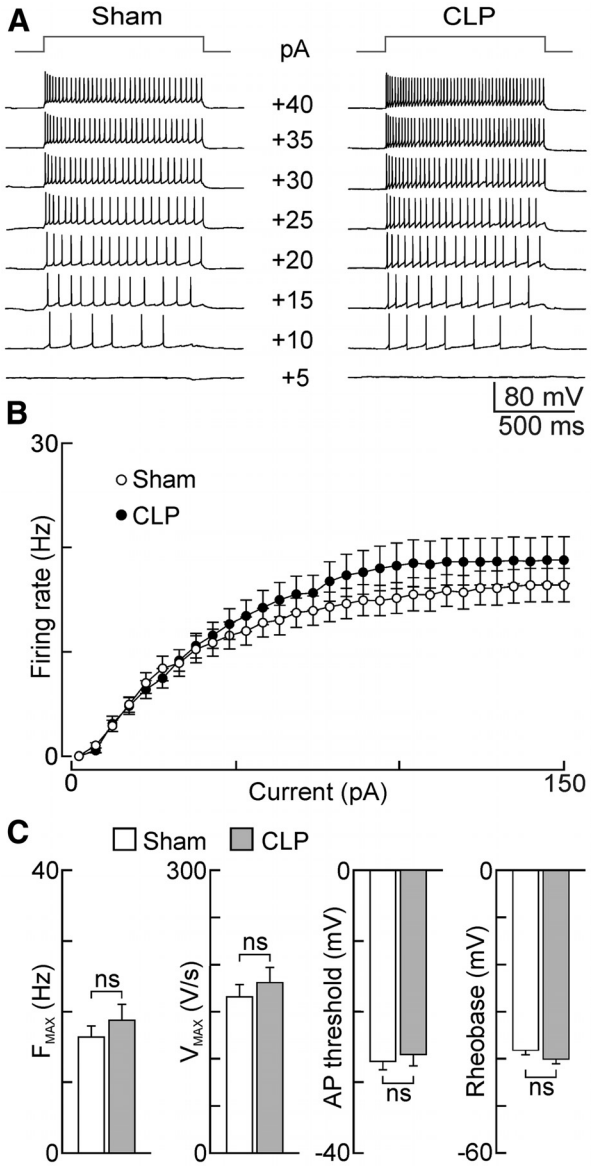

Figure 5. Effects of CLP on the intrinsic excitability of OVLT neurons. ***A***, Traces show voltage responses (bottom) to current pulses (top; intensity indicated next to voltage sweeps) recorded in single OVLT neurons in slices from sham and CLP animals. ***B***, Plots show mean ± SEM steady-state frequencies recorded during the second half of a 1 s pulse in the two groups of neurons (sham, $n = 25$ neurons/6 rats; CLP, $n = 24$ neurons/6 rats). ***C***, Bar graphs show mean ± SEM values of F_{MAX} (sham, $n = 25$ neurons/6 rats; CLP, $n = 24$ neurons/6 rats), as well as V_{MAX}, AP threshold, and rheobase (sham, $n = 22$ neurons/3 rats; CLP, $n = 21$ neurons/3 rats for the latter 3 parameters) observed in the two groups of cells under current clamp. ns, not significant.

lamic explants at one of seven predefined positions mapped over the core region of the OVLT (Fig. 3*A*). The electrode was then advanced from the surface of the tissue to a final depth of 300 μm, and the total number of spontaneously active neurons encountered along the track was registered for each position. As illustrated in Figure 3*B*, the density of spontaneously active neurons observed in CLP rats (0.75 ± 0.11 neurons/track; $n = 56$ tracks) was significantly lower than in shams (1.50 ± 0.23 neurons/track; $n = 28$ tracks; $p = 0.00112$, *t* test). Although the average basal firing rate of OVLT neurons recorded in CLP explants was slightly lower than that observed in shams, this effect was not statistically significant (sham, 2.8 ± 0.34 Hz, $n = 54$; CLP, 1.94 ± 0.28 Hz, $n = 55$; $p = 0.0586$; Fig. 3*C*).

Previous work has shown that sepsis induced by the CLP procedure can induce signs of apoptosis in the median preoptic nucleus (Kafa et al., 2010), a structure that lies immediately dorsal to the OVLT. Therefore, we examined whether the reduced density of active neurons in the OVLT of septic rats might be attributable to neuronal loss. To test this hypothesis, we compared the density of OVLT cells stained with the neuronal marker NeuN in tissue sections (sham, $n = 26$ sections from 3 rats; CLP, $n = 23$ sections from 3 rats). However, as illustrated in Figure 3*D*, the average density of NeuN-stained neurons counted in the OVLT was not different between the two groups of animals ($p = 0.333$; Fig. 3*E*).

We next examined the membrane properties of OVLT neurons using whole-cell patch-clamp recordings in hypothalamic slices prepared from septic and sham animals. As illustrated in Figure 4*A–C*, steady-state *I–V* analysis showed that OVLT neurons from CLP animals display a significantly more hyperpolarized RMP than shams (sham, −40.1 ± 2.3 mV, $n = 23$; CLP, −47.8 ± 2.4 mV, $n = 22$; $p = 0.0266$, *t* test; Fig. 4*C*). Regression analysis in the linear region of the *I–V* indicated that membrane conductance was significantly lower in neurons from CLP animals compared with shams (sham, 1.299 ± 0.050 nS; CLP, 0.915 ± 0.069 nS; $p = 0.0479$; Fig. 4*C*).

Although the more negative resting potential of OVLT neurons in CLP rats could explain why fewer neurons display spontaneous electrical activity, this effect could also be caused by a relative decrease in the intrinsic excitability of the cells. To determine whether the excitability of OVLT neurons was affected by the CLP procedure, frequency–current (*F–I*) analysis was performed under current clamp. For this procedure, the baseline voltage of every cell was first adjusted to a subthreshold value near −60 mV by continuous current injection. We then examined the effects of superimposing a series of 1 s depolarizing pulses whose amplitude increased consecutively by 5 pA (pulse rate, 0.1 Hz). As illustrated in Figure 5*A–C*, there were no significant differences in

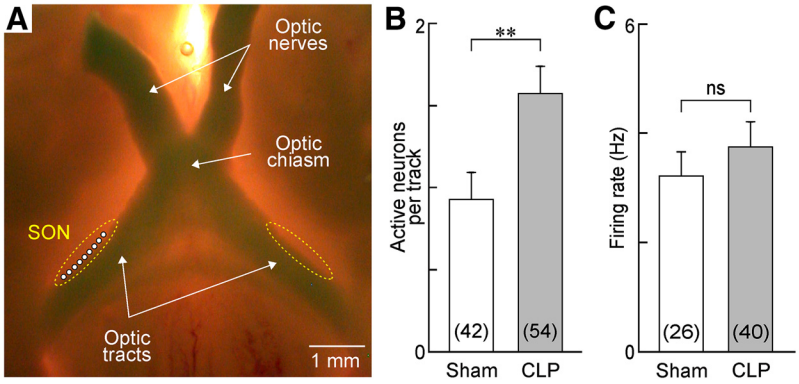

Figure 6. Sepsis increases spontaneous electrical activity of MNCs in the SON. ***A***, Whole-mount photograph showing the ventral surface of a hypothalamic explant configured for extracellular recording from MNCs in the SON (dotted lines). Top is rostral, and bottom is caudal. All recordings were made immediately lateral to the optic tract at the positions indicated by the white circles. ***B***, Bar graph shows the mean ± SEM density of spontaneously active MNCs recorded in the SON of explants prepared from sham (n = 42 tracks/5 rats) and CLP (n = 54 tracks/6 rats) animals. ***C***, Bar graph shows the mean ± SEM values of firing frequency of spontaneously firing MNCs (sham, n = 26 neurons/5 rats; CLP, n = 40 neurons/6 rats). **$p < 0.01$; ns, not significant.

the degree of current-induced firing or AP parameters between OVLT neurons from CLP and sham animals. Notably, the maximum firing frequency (F_{MAX}) achieved in each group was not significantly different (sham, 16.4 ± 1.6 Hz, n = 25 neurons; CLP, 18.8 ± 2.3 Hz, n = 24 neurons; p = 0.387), nor were maximal AP upstroke velocity (V_{MAX}: sham, 165.6 ± 13.1 V/s, n = 22 neurons; CLP, 180.8 ± 16.1 V/s, n = 21 neurons; p = 0.465; Fig. 5*C*), AP threshold (sham, −27.0 ± 1.2 mV, n = 22 neurons; CLP, −26.1 ± 1.7 mV, n = 21 neurons; p = 0.650), and rheobase (sham, −38.2 ± 0.95 mV, n = 22 neurons; CLP, −40.1 ± 0.97 mV, n = 21 neurons; p = 0.171).

Effects of sepsis on MNCs

Previous work has shown that circulating AVP levels are increased during the early phase of sepsis in both humans (Sharshar et al., 2003) and rats (Pancoto et al., 2008). Although peak AVP levels are normally attained ~4 h after the CLP procedure in rats, significantly elevated AVP levels have been observed as long as 18–24 h after surgery (Athayde et al., 2009; Martins et al., 2011). Because AVP release from the neurohypophysis is regulated by the electrical activity of MNCs (Dreifuss et al., 1971), an increase in circulating hormone levels could be caused by an increase in the proportion of electrically active MNCs and/or by an increase in the firing rate of these neurons (Bourque, 1991). Therefore, we compared the spontaneous electrical activity of MNCs in the SON of hypothalamic explants prepared from CLP and sham animals. Extracellular recordings of single-unit AP firing were obtained by advancing an electrode at a rate of 0.4 μm/s to a maximum depth of 200 μm along nine positions per rat within the core region of the SON (Fig. 6*A*). As shown in Figure 6*B*, the average density of spontaneously active neurons was significantly greater in the SON of CLP rats compared with shams (sham, 0.93 ± 0.17 neurons/track, n = 42 tracks; CLP, 1.57 ± 0.17 neurons/track, n = 54 tracks; p = 0.008, t test). The average firing rate of spontaneously active MNCs was slightly greater in CLP rats, but this effect was not statistically significant (sham, 3.7 ± 0.63 Hz, n = 26; CLP, 4.3 ± 0.7 Hz, n = 40; p = 0.551; Fig. 6*C*).

We next examined the effects of CLP on the membrane properties of SON MNCs using whole-cell voltage- and current-clamp recording in hypothalamic slices. As illustrated in Figure 7, *A* and *B*, MNCs from CLP animals displayed *I–V* relations that were similar to those in sham animals. Although the average RMP of MNCs was slightly more positive in CLP animals than in shams, this effect was not significant (sham, −49.9 ± 1.5 mV, n = 47 neurons; CLP, −47.2 ± 1.3 mV, n = 50 neurons; p = 0.177; Fig. 7*C*). The average conductance of the neurons was also unaffected by sepsis (sham, 2.04 ± 0.12 nS, n = 42; CLP, 2.09 ± 0.17 nS, n = 48; p = 0.831; Fig. 7*C*). *F–I* analysis performed under current clamp revealed that MNCs from CLP animals (n = 22) were significantly less responsive than shams (n = 23) in a narrow range of current injection (25–45 pA; $p < 0.05$, t test; Fig. 8*A*,*B*). Consistent with this finding, we found that rheobase was significantly more positive in MNCs from septic rats (sham, −47.6 ± 0.56 mV, n = 24; CLP, −45.6 ± 0.60 mV, n = 22; p = 0.0219, t test; Fig. 8*C*). However, none of the other parameters analyzed were significantly different: F_{max} (sham, 46.8 ± 1.8 Hz, n = 22; CLP, 44.5 ± 1.8 Hz, n = 21; p = 0.372); V_{max} (sham, 193.04 ± 12.8 V/s, n = 25; CLP, 208.48 ± 12.6 V/s, n = 26; p = 0.394; Fig. 8*C*), and AP threshold (sham, −33.9 ± 0.82 mV, n = 25; CLP, −33.8 ± 0.77 mV, n = 26; p = 0.963).

Last, we examined whether the osmoresponsiveness of MNCs was affected using extracellular recordings from SON neurons in hypothalamic explants. As illustrated in Figure 9*A–D*, MNCs recorded in explants from sham and CLP rats both displayed significant increases in firing rate in response to a hyperosmotic stimulus (sham, from 2.96 ± 0.64 to 6.77 ± 0.94 Hz, n = 19, t = 4.662, $p < 0.001$; CLP, from 2.15 ± 0.56 to 4.58 ± 0.82 Hz, n = 20; t = 3.092, $p < 0.016$; one-way repeated measures ANOVA and Holm–Sidak *post hoc* test). Although the proportion of osmoresponsive cells was not different in the two groups (sham, 94.7%; CLP, 80%; p = 0.342, χ^2 test; Fig. 9*E*), the average firing rate observed in the hyperosmotic condition was significantly lower in MNCs from CLP animals compared with shams (t = 2.697, p = 0.028, Holm–Sidak test; Fig. 9*D*).

Discussion

The effects of sepsis on brain function have a significant influence on the quality of life of patients that survive septic shock (Lazosky et al., 2010; Sonneville et al., 2013; Ziaja, 2013), yet little is known about how sepsis affects the electrical properties of central neurons. Here we used a rodent CLP model that approximates human peritoneal sepsis (Rittirsch et al., 2009; Dejager et al., 2011) to investigate how hypothalamic neurons responsible for hydromineral homeostasis are affected during this condition. Our experiments specifically examined the cellular and behavioral changes associated with the acute phase of untreated sepsis, which occurs 18–24 h after surgery in rats (Pancoto et al., 2008; Oliveira-Pelegrin et al., 2009; Rittirsch et al., 2009).

Previous studies showed that systemic infusion of endotoxins can inhibit thirst induced by water deprivation through an effect involving the preoptic area (Calapai et al., 1990; Wang and Evered, 1993; Nava and Carta, 2000). Because this region encompasses the central osmoreceptor (OVLT), these observations suggested that osmotic thirst might become impaired during sepsis. Indeed, our results reveal that thirst stimulated by systemic hypertonicity is impaired during acute sepsis. In agreement with the loss of this behavioral response *in vivo*, we observed that the

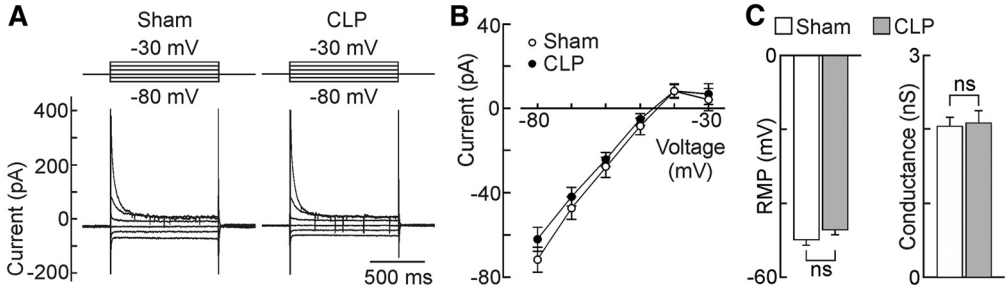

Figure 7. Effects of sepsis on the membrane properties of SON neurons. ***A***, Whole-cell membrane current responses (bottom) to voltage commands (top) recorded from MNCs in the SON of hypothalamic slices. Each set of traces shows the average responses generated by the entire set of sham ($n = 23$ neurons/2 rats) and CLP ($n = 28$ neurons/3 rats) neurons studied. ***B***, Average *I–V* plots obtained from the corresponding cells. ***C***, Bar graphs show mean ± SEM values of RMP and conductance (sham, $n = 47$ neurons/6 rats; CLP, $n = 50$ neurons/6 rats) in the two groups of animals. ns, not significant.

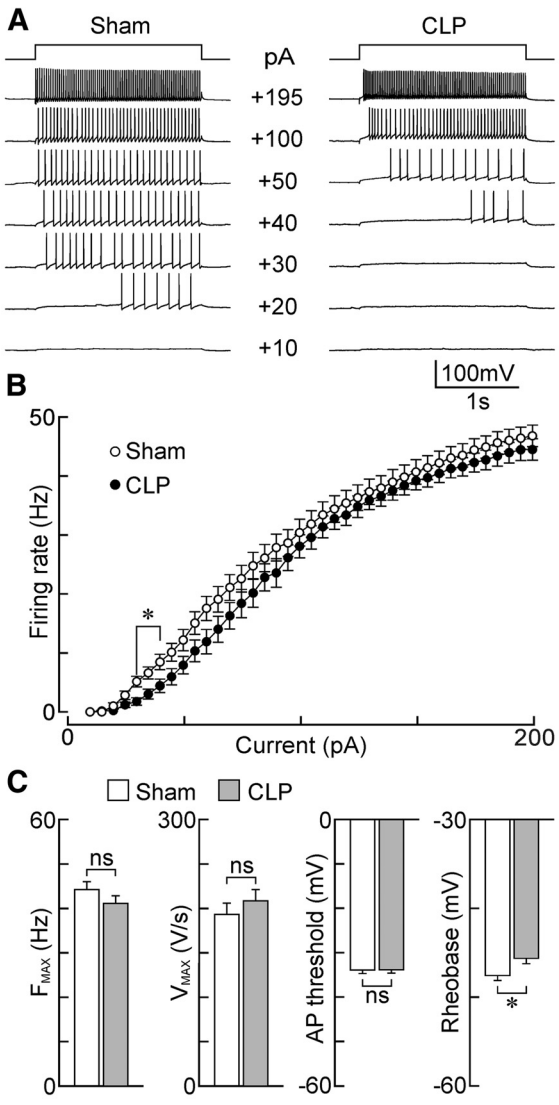

Figure 8. Effects of sepsis on the intrinsic excitability of MNCs. ***A***, Voltage responses of single MNCs (bottom traces) to current steps (top; intensity indicated next to each voltage sweep) in the SON of slices from sham (left) and CLP (right) animals. ***B***, Plots show mean ± SEM steady-state firing rate induced as a function of current in MNCs from shams ($n = 22$ neurons/4 rats) and CLP ($n = 21$ neurons/3 rats) animals. ***C***, Bar graphs show the mean ± SEM values of various parameters related to intrinsic excitability in MNCs from sham and CLP rats: F_{MAX} (sham, $n = 22$ neurons/4 rats; CLP, $n = 21$ neurons/3 rats), V_{MAX} (sham, $n = 25$ neurons/4 rats; CLP, $n = 26$ neurons/4 rats), AP threshold (sham, $n = 25$ neurons/4 rats; CLP, $n = 26$ neurons/4 rats), and rheobase (sham, $n = 24$ neurons/4 rats; CLP, $n = 22$ neurons/3 rats). $^*p < 0.05$; ns, not significant.

responsiveness of OVLT neurons to hyperosmotic stimulation *in vitro* was severely compromised. This impaired osmoresponsiveness of OVLT neurons may be a causal factor in the loss of thirst and osmoregulatory defects associated with the acute phase of sepsis.

Approximately 65% of OVLT neurons are excited by exposure to hyperosmotic fluid, and this response is mediated in part by the activation of ion channels encoded by the transient receptor potential vanilloid type 1 (*trpv1*) gene (Ciura and Bourque, 2006; Bourque et al., 2007; Ciura et al., 2011). The data reported here show that the proportion of osmoresponsive neurons declines significantly during sepsis and that the excitatory effect of hyperosmotic stimulation on osmosensitive OVLT neurons is impaired dramatically in explants prepared from septic animals. Moreover, the density of OVLT neurons displaying spontaneous AP firing under resting conditions was reduced significantly in explants prepared from CLP rats. This observation is significant because the excitatory drive to downstream osmoregulatory effector neurons, such as MNCs, is likely mediated by the global activity of afferent OVLT neurons. Indeed, the increase in firing rate observed in OVLT neurons exposed to hypertonicity is relatively small (e.g., ~1 Hz for a 15 mOsm/kg stimulus; Fig. 2*D*), and many of the cells in this nucleus are silent under control conditions and become electrically active when stimulated by hypertonicity (Ciura and Bourque, 2006). Therefore, the effect of hypertonicity on the firing rate of effector neurons is likely to reflect the integrated synaptic information provided by a large pool of OVLT neurons.

Previous studies have shown that expression of the immediate early gene *Fos* is increased in the OVLT after systemic injections of lipopolysaccharide (Rivest and Laflamme, 1995; Xia and Krukoff, 2001; du Plessis et al., 2006; Corrêa et al., 2007). Although this suggests that OVLT neurons may be excited during sudden exposure to endotoxin, these data do not provide information regarding the time course or persistence of changes in electrical activity or excitability. Our results indicate that OVLT neurons are inhibited 18–24 h after sepsis is established by CLP. Additional studies are needed to examine the effect of CLP at earlier and later time points during electrophysiological recordings from OVLT neurons.

The effects of CLP on the electrophysiological properties of OVLT neurons and osmotically induced thirst are consistent with studies showing that global lesions of the OVLT abolish osmotic thirst in rats (Johnson and Buggy, 1978; Thrasher and Keil, 1987) and other mammals (Thrasher et al., 1982; McKinley et al., 1992). Although the basis for the loss of osmoresponsiveness in OVLT neurons remains to be determined, possible causes

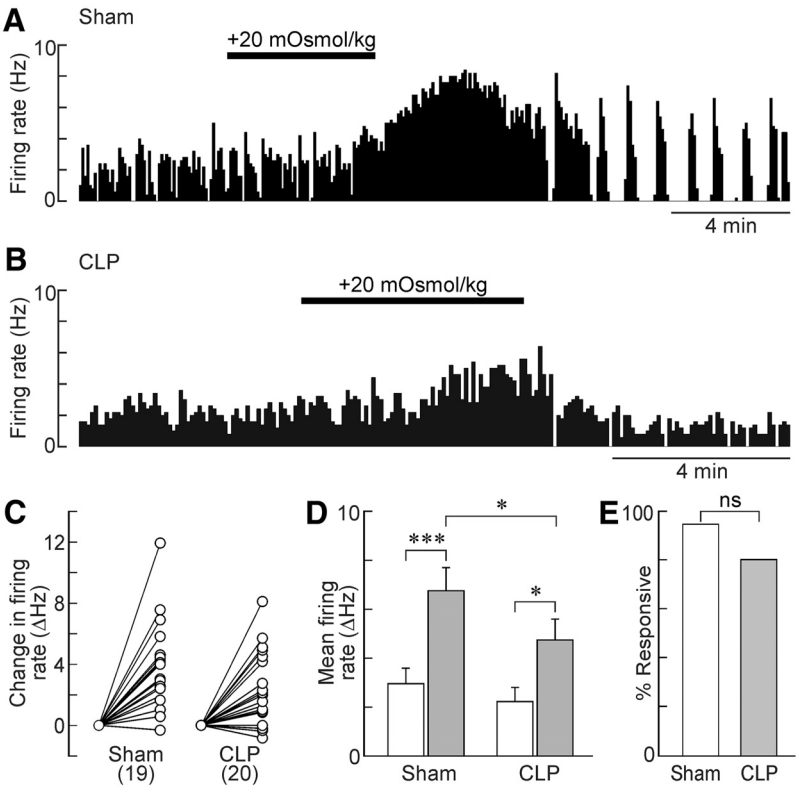

Figure 9. Effects of sepsis on osmoresponsiveness in MNCs. ***A***, Ratemeter record showing the firing rate of a single SON neuron subjected to hyperosmotic stimulation (bar) in an explant prepared from a sham rat. ***B***, Representative response of an SON neuron recorded from an explant obtained from a CLP rat. ***C***, Two-point plots show the changes in firing rate induced by hyperosmotic stimulation in all of the SON neurons tested in sham ($n = 19$ neurons/5 rats) and CLP ($n = 20$ neurons/5 rats) rats. ***D***, Bar graphs show mean ± SEM values of firing rate observed before (white bars) and during (gray bars) a hyperosmotic stimulus for the cells plotted in ***C***. ***E***, Bar graph shows percentage of responders in sham and CLP animals. $^*p < 0.05$; $^{***}p < 0.001$; ns, not significant.

include a decrease in the expression of the Trpv1 channels required for osmoreception (Ciura and Bourque, 2006) or an impairment of elements that mechanically couple osmotically induced changes in cell volume to channel activation (Zhang and Bourque, 2003; Zhang et al., 2007; Ciura et al., 2011; Prager-Khoutorsky et al., 2014).

Our electrophysiological recordings from OVLT neurons in hypothalamic slices provide some insight into the mechanism responsible for the reduced density of electrically active neurons observed in the OVLT of septic rats. Although the ability to fire APs and the intrinsic excitability of OVLT neurons did not seem to differ in sham and CLP-treated rats, the RMP of the cells was significantly hyperpolarized in the septic condition. In fact, many of the cells were hyperpolarized to voltages well below rheobase, explaining why an increased fraction of OVLT neurons were silent under these conditions. *I–V* analysis indicated that the hyperpolarized RMP of OVLT neurons in septic rats was associated with a decrease in slope conductance. Moreover, the reversal potential for this effect, obtained by extrapolating the linear regressions, was near −24 mV (data not shown). These observations suggest that the hyperpolarization of septic OVLT neurons is attributable to the inhibition of a tonic nonselective cation current (Oliet and Bourque, 1993; Voisin et al., 1999). The identity of the ion channel or channels modulated during sepsis, as well as the mediators of these effects, remain to be established. It is interesting to note that the inhibitory effect of endotoxin on water intake can be mimicked by application of tumor necrosis factor α within the preoptic area (Calapai et al., 1994). Because the OVLT is a circumventricular organ that lacks a blood–brain barrier, circulating proinflammatory cytokines would likely have ready access to these neurons.

Because the acute phase of CLP is associated with an increase in circulating AVP levels, we also examined the effects of CLP on the properties of hypothalamic MNCs whose electrical activity determines secretion by the neurohypophysis (Dreifuss et al., 1971; Bourque, 1991). However, whole-cell recordings from MNCs in slices did not reveal any changes in membrane properties that could explain an increase in the electrical excitability of these neurons in animals subjected to CLP. In fact, MNCs were slightly less excitable because of a depolarization of rheobase. Moreover, the AP firing rate of osmotically stimulated MNCs was significantly lower in preparations from CLP animals than in shams. Although the basis for the latter changes remains to be determined, it can be concluded that changes in the intrinsic properties of MNCs do not appear to be responsible for enhanced AVP release during the acute phase of sepsis.

Interestingly, extracellular recordings from MNCs in hypothalamic explants indicated that a significantly greater proportion of these cells are electrically active under basal conditions in CLP animals compared with shams. This observation suggests that substances released by astrocytes, microglia, or other neurons may enhance the proportion of electrically active neurons in this preparation. Although an increase in the density of spontaneously active MNCs could suffice to increase circulating AVP (Walters and Hatton, 1974; Brimble and Dyball, 1977), it remains possible that CLP provokes an increase in the firing rate of these neurons *in vivo* because of the presence of additional factors. For example, AVP-releasing MNCs are intrinsically thermosensitive (Sharif-Naeini et al., 2008; Sudbury et al., 2010; Sudbury and Bourque, 2013), and it is possible that this property mediates an additional excitatory influence during the febrile response associated with CLP-mediated sepsis (Oliveira-Pelegrin et al., 2009). MNCs are also excited by afferents that relay the hypovolemic condition (Cunningham et al., 2002), and previous studies have shown that hypovolemia can induce long-lasting changes in network properties that affect MNCs (Kuzmiski et al., 2009). Thus, additional studies are required to define the mediators of CLP-induced changes in osmoregulatory neurons and networks.

Last, it is worth mentioning that a previous study reported that sepsis reduces immunohistochemical expression of AVP in SON MNCs, whereas expression is increased in MNCs of the paraventricular nucleus (PVN; Sonneville et al., 2010). These differences were not accompanied by changes in AVP mRNA assessed by *in situ* hybridization, suggesting that they reflect differences in posttranscriptional peptide processing. Whether CLP causes differences in AVP synthesis, degradation, transport, or local release within the SON and PVN remains to be determined.

Concluding remarks

Our data provide insights into the cellular mechanisms that underlie defects in centrally mediated osmoregulatory behaviors and humoral responses during the acute phase of sepsis in rats. A recent study showed that the post-acute phase of septic shock in humans that survive sepsis is commonly associated with a long-lasting deficit in both osmotically evoked thirst and AVP release (Siami et al., 2010, 2013). It is presently unclear why the osmosensitivity of MNCs is preserved while that of OVLT neurons is compromised during the early stages of sepsis. However, as noted previously, the OVLT lacks a blood–brain barrier and neurons in this area may receive immediate exposure to the systemic signals that mediate the deleterious effects of CLP. It will be interesting to determine whether OVLT neurons are permanently compromised after CLP and whether the properties and osmoresponsiveness of MNCs are ultimately affected to impair AVP release during the post-acute phase of sepsis.

References

Angus DC, van der Poll T (2013) Severe sepsis and septic shock. N Engl J Med 369:840–851. CrossRef Medline

Antunes-Rodrigues J, de Castro M, Elias LL, Valença MM, McCann SM (2004) Neuroendocrine control of body fluid metabolism. Physiol Rev 84:169–208. CrossRef Medline

Athayde LA, Oliveira-Pelegrin GR, Nomizo A, Faccioli LH, Rocha MJ (2009) Blocking central leukotrienes synthesis affects vasopressin release during sepsis. Neuroscience 160:829–836. CrossRef Medline

Bauhofer A, Schwarting RK, Köster M, Schmitt A, Lorenz W, Pawlak CR (2004) Sickness behavior of rats with abdominal sepsis can be improved by antibiotic and G-CSF prophylaxis in clinic modeling randomized trials. Inflamm Res 53:697–705. CrossRef Medline

Bourque CW (1991) Activity-dependent modulation of nerve terminal excitation in a mammalian peptidergic system. Trends Neurosci 14:28–30. CrossRef Medline

Bourque CW (2008) Central mechanisms of osmosensation and systemic osmoregulation. Nat Rev Neurosci 9:519–531. CrossRef Medline

Bourque CW, Ciura S, Trudel E, Stachniak TJ, Sharif-Naeini R (2007) Neurophysiological characterization of mammalian osmosensitive neurones. Exp Physiol 92:499–505. CrossRef Medline

Brimble MJ, Dyball RE (1977) Characterization of the responses of oxytocin- and vasopressin-secreting neurones in the supraoptic nucleus to osmotic stimulation. J Physiol 271:253–271. CrossRef Medline

Calapai G, Squadrito F, Massi M, Caputi AP, de Caro G (1990) Endotoxin inhibition of drinking behaviour in the rat. Pharmacol Res 22:161–170. CrossRef Medline

Calapai G, Mazzaglia G, Cilia M, Zingarelli B, Squadrito F, Caputi AP (1994) Mediation by nitric oxide formation in the preoptic area of endotoxin and tumour necrosis factor-induced inhibition of water intake in the rat. Br J Pharmacol 111:1328–1332. CrossRef Medline

Cinel I, Opal SM (2009) Molecular biology of inflammation and sepsis: a primer. Crit Care Med 37:291–304. CrossRef Medline

Ciura S, Bourque CW (2006) Transient receptor potential vanilloid 1 is required for intrinsic osmoreception in organum vasculosum lamina terminalis neurons and for normal thirst responses to systemic hyperosmolality. J Neurosci 26:9069–9075. CrossRef Medline

Ciura S, Liedtke W, Bourque CW (2011) Hypertonicity-sensing in organum vasculosum lamina terminalis neurons: a mechanical process involving Trpv1 but not Trpv4. J Neurosci 31:14669–14676. CrossRef Medline

Corrêa PB, Pancoto JA, de Oliveira-Pelegrin GR, Cárnio EC, Rocha MJ (2007) Participation of iNOS-derived NO in hypothalamic activation and vasopressin release during polymicrobial sepsis. J Neuroimmunol 183:17–25. CrossRef Medline

Cunningham JT, Bruno SB, Grindstaff RR, Grindstaff RJ, Higgs KH, Mazzella D, Sullivan MJ (2002) Cardiovascular regulation of supraoptic vasopressin neurons. Prog Brain Res 139:257–273. Medline

Dejager L, Pinheiro I, Dejonckheere E, Libert C (2011) Cecal ligation and puncture: the gold standard model for polymicrobial sepsis? Trends Microbiol 19:198–208. CrossRef Medline

Dreifuss JJ, Kalnins I, Kelly JS, Ruf KB (1971) Action potentials and release of neurohypophysial hormones in vitro. J Physiol 215:805–817. CrossRef Medline

du Plessis I, Mitchell D, Niesler C, Laburn HP (2006) c-Fos immunoreactivity in selected brain regions of rats after heat exposure and pyrogen administration. Brain Res 1120:124–130. CrossRef Medline

Giusti-Paiva A, Santiago MB (2010) Neurohypophyseal dysfunction during septic shock. Endocr Metab Immune Disord Drug Targets 10:247–251. CrossRef Medline

Hart BL (1988) Biological basis of the behavior of sick animals. Neurosci Biobehav Rev 12:123–137. CrossRef Medline

Hollis JH, McKinley MJ, D'Souza M, Kampe J, Oldfield BJ (2008) The trajectory of sensory pathways from the lamina terminalis to the insular and cingulate cortex; a neuroanatomical framework for the generation of thirst. Am J Physiol Regul Integr Comp Physiol 294:R1390–R1401. CrossRef Medline

Johnson AK (2007) The sensory psychobiology of thirst and salt appetite. Med Sci Sports Exerc 39:1388–1400. CrossRef Medline

Johnson AK, Buggy J (1978) Periventricular preoptic-hypothalamus is vital for thirst and normal water economy. Am J Physiol 234:R122–R129. Medline

Jones CW, Pickering BT (1969) Comparison of the effects of water deprivation and sodium chloride imbibition on the hormone content of the neurohypophysis of the rat. J Physiol 203:449–458. CrossRef Medline

Kafa IM, Uysal M, Bakirci S, Ayberk Kurt M (2010) Sepsis induces apoptotic cell death in different regions of the brain in a rat model of sepsis. Acta Neurobiol Exp (Wars) 70:246–260. Medline

Kanczkowski W, Alexaki VI, Tran N, Großklaus S, Zacharowski K, Martinez A, Popovics P, Block NL, Chavakis T, Schally AV, Bornstein SR (2013) Hypothalamo-pituitary and immune-dependent adrenal regulation during systemic inflammation. Proc Natl Acad Sci U S A 110:14801–14806. CrossRef Medline

Kuzmiski JB, Pittman QJ, Bains JS (2009) Metaplasticity of hypothalamic synapses following in vivo challenge. Neuron 62:839–849. CrossRef Medline

Lazosky A, Young GB, Zirul S, Phillips R (2010) Quality of life after septic illness. J Crit Care 25:406–412. CrossRef Medline

Martins TF, Sorgi CA, Faccioli LH, Rocha MJ (2011) Leukotriene synthesis inhibitor decreases vasopressin release in the early phase of sepsis. J Neuroimmunol 238:52–57. CrossRef Medline

McKinley MJ, Bicknell RJ, Hards D, McAllen RM, Vivas L, Weisinger RS, Oldfield BJ (1992) Efferent neural pathways of the lamina terminalis subserving osmoregulation. Prog Brain Res 91:395–402. CrossRef Medline

McKinley MJ, Denton DA, Oldfield BJ, De Oliveira LB, Mathai ML (2006) Water intake and the neural correlates of the consciousness of thirst. Semin Nephrol 26:249–257. CrossRef Medline

Nava F, Carta G (2000) Repeated lipopolysaccharide administration produces tolerance to anorexia and fever but not to inhibition of thirst in rat. Int J Immunopharmacol 22:943–953. CrossRef Medline

Oliet SH, Bourque CW (1993) Steady-state osmotic modulation of cationic conductance in neurons of rat supraoptic nucleus. Am J Physiol 265:R1475–R1479. Medline

Oliveira-Pelegrin GR, Ravanelli MI, Branco LG, Rocha MJ (2009) Thermoregulation and vasopressin secretion during polymicrobial sepsis. Neuroimmunomodulation 16:45–53. CrossRef Medline

Pancoto JA, Corrêa PB, Oliveira-Pelegrin GR, Rocha MJ (2008) Autonomic dysfunction in experimental sepsis induced by cecal ligation and puncture. Auton Neurosci 138:57–63. CrossRef Medline

Prager-Khoutorsky M, Khoutorsky A, Bourque CW (2014) Unique interweaved microtubule scaffold mediates osmosensory transduction via physical interaction with TRPV1. Neuron 83:866–878. CrossRef Medline

Richard D, Bourque CW (1995) Synaptic control of rat supraoptic neurones during osmotic stimulation of the organum vasculosum lamina terminalis in vitro. J Physiol 489:567–577. CrossRef Medline

Rittirsch D, Huber-Lang MS, Flierl MA, Ward PA (2009) Immunodesign of experimental sepsis by cecal ligation and puncture. Nat Protoc 4:31–36. CrossRef Medline

Rivest S, Laflamme N (1995) Neuronal activity and neuropeptide gene transcription in the brains of immune-challenged rats. J Neuroendocrinol 7:501–525. CrossRef Medline

Sharif-Naeini R, Ciura S, Bourque CW (2008) TRPV1 gene required for

thermosensory transduction and anticipatory secretion from vasopressin neurons during hyperthermia. Neuron 58:179–185. CrossRef Medline

Sharshar T, Blanchard A, Paillard M, Raphael JC, Gajdos P, Annane D (2003) Circulating vasopressin levels in septic shock. Crit Care Med 31:1752–1758. CrossRef Medline

Siami S, Bailly-Salin J, Polito A, Porcher R, Blanchard A, Haymann JP, Laborde K, Maxime V, Boucly C, Carlier R, Annane D, Sharshar T (2010) Osmoregulation of vasopressin secretion is altered in the postacute phase of septic shock. Crit Care Med 38:1962–1969. CrossRef Medline

Siami S, Polito A, Porcher R, Hissem T, Blanchard A, Boucly C, Carlier R, Annane D, Haymann JP, Sharshar T (2013) Thirst perception and osmoregulation of vasopressin secretion are altered during recovery from septic shock. PLoS One 8:e80190. CrossRef Medline

Sonneville R, Guidoux C, Barrett L, Viltart O, Mattot V, Polito A, Siami S, de la Grandmaison GL, Blanchard A, Singer M, Annane D, Gray F, Brouland JP, Sharshar T (2010) Vasopressin synthesis by the magnocellular neurons is different in the supraoptic nucleus and in the paraventricular nucleus in human and experimental septic shock. Brain Pathol 20:613–622. CrossRef Medline

Sonneville R, Verdonk F, Rauturier C, Klein IF, Wolff M, Annane D, Chretien F, Sharshar T (2013) Understanding brain dysfunction in sepsis. Ann Intensive Care 3:15. CrossRef Medline

Stachniak TJ, Sudbury JR, Trudel E, Choe KY, Ciura S, Bourque CW (2012) Osmoregulatory circuits in slices and en-bloc preparations of rodent hypothalamus. In: Isolated central nervous system circuits (Ballanyi K, ed), pp 211–231. New York: Humana-Springer.

Sudbury JR, Bourque CW (2013) Dynamic and permissive roles of TRPV1 and TRPV4 channels for thermosensation in mouse supraoptic magnocellular neurosecretory neurons. J Neurosci 33:17160–17165. CrossRef Medline

Sudbury JR, Ciura S, Sharif-Naeini R, Bourque CW (2010) Osmotic and thermal control of magnocellular neurosecretory neurons–role of an N-terminal variant of trpv1. Eur J Neurosci 32:2022–2030. CrossRef Medline

Thrasher TN, Keil LC (1987) Regulation of drinking and vasopressin secretion: role of organum vasculosum laminae terminalis. Am J Physiol 253:R108–R120. Medline

Thrasher TN, Keil LC, Ramsay DJ (1982) Lesions of the organum vasculosum of the lamina terminalis (OVLT) attenuate osmotically-induced drinking and vasopressin secretion in the dog. Endocrinology 110:1837–1839. CrossRef Medline

Trudel E, Bourque CW (2010) Central clock excites vasopressin neurons by waking osmosensory afferents during late sleep. Nat Neurosci 13:467–474. CrossRef Medline

Voisin DL, Chakfe Y, Bourque CW (1999) Coincident detection of CSF Na+ and osmotic pressure in osmoregulatory neurons of the supraoptic nucleus. Neuron 24:453–460. CrossRef Medline

Walters JK, Hatton GI (1974) Supraoptic neuronal activity in rats during five days of water deprivation. Physiol Behav 13:661–667. CrossRef Medline

Wang K, Evered MD (1993) Endotoxin stimulates drinking in rats without changing dehydrational signals controlling thirst. Am J Physiol 265:R1043–R1051. Medline

Xia Y, Krukoff TL (2001) Cardiovascular responses to subseptic doses of endotoxin contribute to differential neuronal activation in rat brain. Brain Res Mol Brain Res 89:71–85. CrossRef Medline

Zhang Z, Bourque CW (2003) Osmometry in osmosensory neurons. Nat Neurosci 6:1021–1022. CrossRef Medline

Zhang Z, Kindrat AN, Sharif-Naeini R, Bourque CW (2007) Actin filaments mediate mechanical gating during osmosensory transduction in rat supraoptic nucleus neurons. J Neurosci 27:4008–4013. CrossRef Medline

Ziaja M (2013) Septic encephalopathy. Curr Neurol Neurosci Rep 13:383. CrossRef Medline